Sensor selection for load estimation of a wind turbine pitch bearing

N. Dwek [1,2], **B. Blockmans** [1,2], **J. Croes** [1,2], **B. Pluymers** [1,2], **M. Kirchner** [1,2]
[1] KU Leuven, Department of Mechanical Engineering,
Celestijnenlaan 300, B-3001, Heverlee, Belgium
e-mail: **nathan.dwek@kuleuven.be**

[2] DMMS Core lab, Flanders Make, Belgium

Abstract
This article tackles sensor selection for the identification of the loads acting on a wind turbine pitch bearing. Virtual sensing is used to estimate those loads, by combining measurements from strain gauges and accelerometers at practical locations with a reduced-order finite element model of the system. This article proposes to work within an Augmented Kalman Filtering (AKF) framework which allows to analytically derive the asymptotic uncertainty on the estimation. This provides a good metric for the performance of a given sensor set and a good basis for the objective function for the sensor selection problem. This optimization problem is combinatorial, with discrete decision variables and a black-box objective function. To approach optimality, a large number of minimal sensor sets are evaluated and the best performing ones are then combined and pruned to obtain an optimized sensor set. The presented approach outperforms hand-picked sensor sets using typical heuristics while remaining consistent with highly excited regions around the pitch bearing.

1 Introduction

This article tackles sensor selection for the identification of the loads acting on a wind turbine pitch bearing. Wind turbines are playing a key role in the transition towards renewable energy sources, and are becoming more and more attractive in terms of return on investment as they scale up in size and nominal power. This scaling up poses new challenges for all wind turbine components (structure, blades, electromechanical drivetrain, ...) and at all stages of their life (manufacturing, resistance to peak loads as well as to wear and fatigue, maintenance, ...).

As a result, little experimental data is available for the combination of new designs and materials that are being deployed at larger and larger scales. This is a first motivation for sensorization and in particular for load identification of wind turbine components, as the data collected during operation can help better understand the current generations and improve the future ones [1].

Optimizing the maintenance of wind turbines or, more globally, of wind farms, is also a key ingredient to attain a unit energy price competitive with other energy sources, and this is a second motivation for applying load identification and, in a wider sense, condition monitoring to this use-case. This is because wind turbines mainly operate in harsh, remote environments (offshore, wind swept plains, in presence of humidity, sand and salt, ...) and require expensive techniques and equipment for access. Downtime is costly and complete failure is catastrophic. As a result, predictive maintenance is essential and must be fully integrated in the operation of a wind farm. This again requires data collection and, more widely, condition monitoring [2, 3].

This paper focuses on a wind turbine pitch bearing, which connects a blade to the rotor and allows it to rotate about its longitudinal axis to change its pitch, i.e. adjust the drag and lift of the blade to control the rotation speed and harnessed wind power. Due to their position in the load path, pitch bearings are subject to harsh cyclic and non-cyclic loads, due to the weight and inertia of the blade itself as it rotates, and to the lift and drag forces generated by the wind. Bearings are omnipresent in a wind turbine as well as in rotating

machinery in general, and bearing condition monitoring is an active research topic in academia and industry with very concrete demands and applications [4, 5]. In wind turbines, bearing condition monitoring is of particular interest for the reasons presented above in this introduction [6]. Load estimation constitutes a first step towards that broader goal and is the topic of this article.

Direct measurement of the load(s) acting on a mechanical structure is not desirable in many applications. Installing transducers in the load path is often impractical or too expensive and is intrusive because it affects the response of the sensorized system to the measured load(s). These considerations weigh even heavier for in-service data collection on a large number of deployed systems. In the case of bearings, mounting force cells or strain gauges on or close to the raceways and rolling elements is close to impossible, even though in situ strain measurement using fiber Braggs gratings has been suggested [7, 8]. As a result, indirect load identification is the predominant state of practice and is considered in this article.

More generally, virtual sensing allows to estimate quantities that are too costly or difficult to directly measure, by combining measurements from more practical sensors and locations with models of the system in question. In the case of load estimation, this involves solving an inverse problem to obtain input forces starting from output strains, displacements or accelerations at given locations on the structure. This is not straightforward, and multiple approaches have been proposed in the time or frequency-domain [9, 10, 11]. This article considers load estimation using an Augmented Kalman Filter (AKF) [12, 13], which is the most commonly used estimation algorithm for this application. The motivation behind this choice and some specifics on the implementation are detailed further in section 2. For now, this introduction concludes by presenting the problem of sensor selection for virtual sensing, and why this topic on its own is of particular interest.

The key feature of virtual sensing is that it allows to use indirect measurements with relative freedom on the position of the sensors. In turn, this makes the selection and placement of these sensors less obvious as more decision criteria can be taken into account. Because estimation techniques typically do not provide a forward, explicit relation from measurements to the estimated quantities, and instead rely on (recursive) filtering or on optimization over a certain horizon, it is rarely possible to rigorously derive hard and fast rules on sensor selection for a given virtual sensing use-case. Despite those considerations, sensor selection is crucial to the performance and cost of a virtual sensing solution. Typically, the design and performance of the estimator depends on the choice of sensors while the sensors are chosen based on estimator performance. Because of this circular dependency, an initial suggestion of sensor set made independently of any existing estimator is valuable, and has been the subject of multiple investigations in the past [14, 15, 16, 17, 18, 19, 20]. This is why the selection of sensors for the use-case of load estimation of a wind turbine pitch bearing is treated here as its own topic.

This article is organized as follows. Section 2 motivates the usage of Kalman Filtering as a framework for sensor selection, briefly introduces Augmented Kalman Filtering and the associated notations, and concludes with the derivation of the covariance matrix $\mathbf{P}_\infty$ of the asymptotic uncertainty on the state estimation, which is used to quantify the performance of a given sensor set. Section 3 presents the procedure to perform the actual sensor selection, based on the above-mentioned performance metric. Section 4 then introduces the use-case on which the proposed sensor selection method is applied, along with the associated models which are inputs to the sensor selection. This leads to section 5 which presents sensor selection results and their performance, with some comparisons to heuristics-based sensor sets. Finally, section 6 concludes this article by drawing the key lessons from this work and by giving some outlooks on future research.

2 Kalman Filtering as a framework for sensor selection

This article works within an AKF framework to predict the performance of a given sensor set. This choice has been made for three reasons:

1. KF-based estimation techniques are strongly established for the considered use-case and for mechatronics applications in general, and they are very widely used, which makes this work relevant to current practices.

2. A KF is the optimal estimator for Linear Time-Invariant (LTI) systems under the assumptions of unbiased additive gaussian noises on the system dynamics and measurements. While these assumptions are often reasonable in mechanical applications, they are not always satisfied and many variations on the core ideas of Kalman Filtering have been demonstrated, such as Extended Kalman Filters (EKF) [21], Unscented Kalman Filters (UKF) [22], Dual Kalman Filters (DKF) [23], and more ad hoc KF-based estimators that handle heavily non-linear and/or time-varying models [16]. However, the fact that optimality might not be guaranteed in realistic use-cases is not a concern for this work because a KF is only used here to derive the uncertainties on the estimated signals resulting from a given choice of sensors, and not to perform the actual estimation itself. Independently of the non-idealities of the system in question and of the eventual choice of estimation strategy, these derived uncertainties provide a strong lower-bound on the uncertainties that can be achieved in practice (*i.e.* an upper-bound on the estimation performance), and as a result form a good criteria for sensor selection [21].

3. Only under the assumptions guaranteeing KF optimality is it possible to theoretically derive estimation uncertainties and asymptotic estimator quantities using Riccati's equation [24] instead of resorting to simulations and/or actually running the proposed estimator. This is crucial for sensor selection as it allows to quickly evaluate many sensor sets. This proposed evaluation method is faster than if it was required to actually run an estimator on training datasets. Moreover, it is based only on the model of the system in question and the positions and accuracies of the individual sensors. In turn, the resulting performance metric is valid in all operating conditions where the model remains accurate, making it a more robust performance metric than using some representative estimation scenario(s).

2.1 Augmented Kalman Filtering and associated notations

This article will not present the detailed derivations of an (A)(E)KF as this topic is very well covered in literature [21, 24, 13, 14], but the notational conventions are introduced below. The underlying dynamical system is modeled in the continuous time using the traditional set of equations (1), where the system matrices may potentially be the result of local linearization around the current state $\mathbf{x}$.

$$\begin{cases} \dot{\mathbf{x}}(t) = \mathbf{A}\mathbf{x}(t) + \mathbf{B}\mathbf{u}(t) + \mathbf{w}(t), & \mathbf{w} \sim \mathcal{N}(\mathbf{0}, \mathbf{Q}) \\ \mathbf{y}(t) = \mathbf{H}\mathbf{x}(t) + \mathbf{D}\mathbf{u}(t) + \mathbf{v}(t), & \mathbf{v} \sim \mathcal{N}(\mathbf{0}, \mathbf{R}) \end{cases} \tag{1}$$

In (1), $\mathbf{A}$ and $\mathbf{B}$ describe the dynamics of the system, $\mathbf{H}$ and $\mathbf{D}$ how the system is observed (*i.e.* types and positions of sensors), and $\mathbf{Q}$ and $\mathbf{R}$ the uncertainties on the input and modeled dynamics (through $\mathbf{w}(t)$) and on the measurements (through $\mathbf{v}(t)$), respectively. Discretization in time is not considered here as it is not necessary for predicting the asymptotic estimation uncertainty resulting from a sensor set, which is the objective of this work. This keeps derivations cleaner and more general.

To perform input estimation and obtain a model that is amenable to Augmented Kalman Filtering, the system state $\mathbf{x}(t)$ is augmented with the input $\mathbf{u}(t)$, resulting in the augmented state-space model (2).

$$\begin{cases} \begin{bmatrix} \dot{\mathbf{x}}(t) \\ \dot{\mathbf{u}}(t) \end{bmatrix} = \begin{bmatrix} \mathbf{A} & \mathbf{B} \\ \mathbf{0} & \mathbf{0} \end{bmatrix} \begin{bmatrix} \mathbf{x}(t) \\ \mathbf{u}(t) \end{bmatrix} + \begin{bmatrix} \mathbf{w}(t) \\ \mathbf{w}_\mathbf{u}(t) \end{bmatrix} \\ \mathbf{y}(t) = \begin{bmatrix} \mathbf{H} & \mathbf{D} \end{bmatrix} \begin{bmatrix} \mathbf{x}(t) \\ \mathbf{u}(t) \end{bmatrix} + \mathbf{v}(t) \end{cases} \tag{2}$$

which is condensed using the following substitutions:

$$\mathbf{x}^* = \begin{bmatrix} \mathbf{x} \\ \mathbf{u} \end{bmatrix}, \quad \mathbf{A}^* = \begin{bmatrix} \mathbf{A} & \mathbf{B} \\ \mathbf{0} & \mathbf{0} \end{bmatrix}, \quad \mathbf{w}^* = \begin{bmatrix} \mathbf{w} \\ \mathbf{w}_\mathbf{u} \end{bmatrix} \quad \mathbf{w}^* \sim \mathcal{N}(\mathbf{0}, \mathbf{Q}^*), \quad \mathbf{H}^* = \begin{bmatrix} \mathbf{H} & \mathbf{D} \end{bmatrix}$$

Matrices $\mathbf{A}^*$ and $\mathbf{H}^*$ are used as the state prediction matrix and measurement matrix of the AKF, respectively.

The final ingredients required to predict the asymptotic estimation uncertainty of the corresponding AKF are the respective covariance matrices for the measurement noise $\mathbf{R}$ and the process noise $\mathbf{Q}^*$. $\mathbf{R}$ is trivial as it is a diagonal matrix of the respective noises of the sensors, which can be based on available sensor

specifications or on experimental data. $\mathbf{Q}^*$ is given some attention here, as this article focuses mostly on manipulating those covariance matrices to the predict estimation uncertainty.

The $\mathbf{Q}$ matrix in model (1) describes the uncertainties on the process model itself (matrices $\mathbf{A}$ and $\mathbf{B}$) as well as on the known input $\mathbf{u}(t)$. For estimation of only the states, based on a known input signal, this $\mathbf{Q}$ matrix is typically the most challenging tuning parameter of the KF. For joint state-input estimation using an AKF, this challenge is slightly different, and some assumptions must be made.

The first and fundamental assumption behind an AKF is to model the dynamics of the unknown input in (2) as a Gaussian random walk associated with a covariance matrix $\mathbf{Q_{uu}}$, as indicated in (3) [21].

$$\mathbf{w_u} \sim \mathcal{N}(\mathbf{0}, \mathbf{Q_{uu}}) \tag{3}$$

The second assumption is that $\mathbf{Q}_{\text{model}} \ll \mathbf{Q_{uu}}$. This is required for input estimation to be feasible and ensure that the measurement innovation — the difference between the actual measurement $\mathbf{y}(t)$ and the predicted measurement $\hat{\mathbf{y}}(t)$ — results in an update in the estimated input and is not wrongly attributed to modeling uncertainties.

This finally results in expression (4) for $\mathbf{Q}^*$.

$$\mathbf{Q}^* = \begin{bmatrix} \mathbf{0} & \mathbf{0} \\ \mathbf{0} & \mathbf{Q_{uu}} \end{bmatrix} \tag{4}$$

This structure of $\mathbf{Q}^*$ is practical in the sense that it eliminates the need for tuning $\mathbf{Q}_{\text{model}}$, but tuning $\mathbf{Q_{uu}}$ remains a challenge, especially as modelling the unknown input $\mathbf{u}(t)$ as a gaussian random walk is a strong assumption that rarely completely fits the actual input. As a result, tuning $\mathbf{Q_{uu}}$ is a compromise between the response delay of the estimator and its sensitivity to noise. $\mathbf{Q_{uu}}$ must be chosen based on which aspects of the input $\mathbf{u}(t)$ must be captured by the estimator [15].

With these models and corresponding matrices at hand, the covariance matrix $\mathbf{P}_\infty$ of the asymptotic uncertainty on the estimated state can be derived. This is the topic of the next subsection.

2.2 Performance of a sensor set within this framework

Under the KF assumptions where optimality is guaranteed, the covariance matrix $\mathbf{P}_\infty$ of the asymptotic uncertainty on the estimated state is given by the solution to the Continuous Algebraic Riccati Equation (CARE) [24].

$$\mathbf{A}^* \mathbf{P}_\infty + \mathbf{P}_\infty \mathbf{A}^{*T} - \mathbf{P}_\infty \mathbf{H}^T \mathbf{R}^{-1} \mathbf{H} \mathbf{P}_\infty + \mathbf{Q}^* = \mathbf{0} \tag{5}$$

The continuous equation is used here because time-discretization is not necessary for sensor selection.

As proposed above, this theoretical value of $\mathbf{P}_\infty$ is used to quantify the performance of a given sensor set. This choice allows to simultaneously account for the signal to noise ratio (SNR) of the sensors and for how they affect the observability of the system [20, 14].

$\mathbf{P}_\infty$ is superior to sensor SNR as a performance metric because it takes into account how the positions and types of sensors impact the information they provide about the states of the system. On the contrary, the practice of selecting sensors purely based on highest SNR can lead to sensor sets that are redundant and/or leave some states unobservable or poorly observable.

$\mathbf{P}_\infty$ is also superior to some sort of observability measure as a performance metric because it takes into account the SNR of each sensor, and because it quantifies in a more natural and rigorous way how the positions and types of sensors impact the information they provide about the states of the system. Observability of the system has been previously proposed as a sensor selection criterion, for example using the Popov-Belevitch-Hautus (PBH) test [15, 20]. Since observability is a fundamentally binary characteristic, workarounds must be used to derive a non-binary metric of performance from it, such as the condition number of the PBH matrix which quantifies how close it is to being rank-deficient. Still, this is contrived compared to using $\mathbf{P}_\infty$ which naturally quantifies the quality of the information provided by the sensors about the states. This

quantification is more rigorous and nuanced as it provides the expected uncertainty per state. Finally, as demonstrated in [14, 15], using the PBH criterion can lead to some sensor types being incorrectly favored if unit scaling and SNR are not properly taken into account. This pitfall is inherently avoided by using $\mathbf{P}_\infty$ as a performance metric.

Quantifying the performance of a given sensor set based on $\mathbf{P}_\infty$ is the first ingredient towards sensor selection. The second and final ingredient is a selection algorithm to explore the space of feasible sensors and arrive at a close to optimal sensor set.

3 Sensor selection algorithm

Sensor selection is a hard optimization problem outside of trivial cases. Because this work uses FE-based models, the decision variables are the nodes at which sensors are placed and the type(s) of sensor(s) per selected node. This makes the optimization problem purely combinatorial with a very large set of discretized positions (*i.e.* nodes) at which sensors are allowed to be placed. Moreover, it has a black-box objective function since no explicit expression can be derived of $\mathbf{P}_\infty$ in function of the decision variables (*i.e.* the selected nodes and sensor types).

3.1 General optimization approach

Given the above-listed characteristics, black-box optimization strategies must be used. In particular, selection strategies that are sequential, backward, and greedy have been demonstrated with success [25, 15, 14]. The sensor selection algorithm used in this work shares those same characteristics and a short explanation on each is presented below:

- *Sequential* selection as opposed to *simultaneous* means that the optimized sensor set is obtained by adding or removing sensors one by one, instead of by attempting to simultaneously place all of them. A sequential strategy is chosen because simultaneous strategies are only feasible for small problem scales due to the combinatorial complexity of the sensor selection problem.
- *Backward* selection as opposed to *forward* means that the optimized sensor set is obtained by removing sensors from a larger set, instead of adding them to a starting empty set. Backward selection is chosen because evaluating $\mathbf{P}_\infty$ requires a minimum set of sensors to ensure observability and to ensure that the CARE admits a stabilizing solution. This excludes starting from an empty set. Moreover, forward selection requires to quantify the amount of information provided by a single sensor s_{j+1} given an existing sensor set $\mathbf{S}_j$. In this work, this is done by comparing $\mathbf{P}_\infty(\mathbf{S}_j)$ to $\mathbf{P}_\infty(\mathbf{S}_j \cup \{s_{j+1}\})$. Backward selection only requires to evaluate this for each sensor in the current sensor set, to the contrary of forward selection which requires to evaluate this for each candidate sensor outside the current set, which is much more computationally demanding.
- *Greedy* selection means that each step removes the sensor that affects performance the least *at that step*. Greedy algorithms do not guarantee optimality of the sensor selection but they are practical for difficult optimization problems like this one and follow reasonable heuristics.

Because greedy approaches only chase local optimality and because backward selection does not allow to expand the search beyond the current set, the choice of initial sensor set has a determining influence on the performance of the optimized sensor set. Some attention is given to this in the following subsection.

3.2 Initial sensor set construction

In previous work [15, 14], the initial sensor set is chosen based on the SNR of individual sensors in training scenarios. Even for sensor pre-selection, the drawbacks of SNR as a selection criterion have been presented above, and it does not provide satisfactory results for the use-case considered in this article. High SNR thresholds lead to initial sensor sets of manageable size but with poor $\mathbf{P}_\infty$ due to the highly excited sensors

being grouped together in a few specific clusters. Lower SNR thresholds lead to initial sensor sets with better geometrical distribution and $\mathbf{P}_\infty$, but with impractical size. Solutions have been proposed to further refine this approach, for example with constraints on the minimum distance between the sensors in the initial sensor set [15, 14].

This article proposes a novel approach to efficiently obtain an initial sensor set of manageable size with good $\mathbf{P}_\infty$. Along with its many qualities listed above, $\mathbf{P}_\infty$ has the downside that it can only be evaluated for sensor sets of a minimum size. As a result, the central idea in this work is to never treat sensors individually. Instead, this article proposes the following approach, which is inspired by quasi Monte Carlo optimization [26].

1. Generate a large number of random sensor sets, each with sufficient size that $\mathbf{P}_\infty$ can be evaluated.
2. Select from this pool of sensor sets the best performing one for each quantity to estimate, *i.e.* for each corresponding diagonal entry of $\mathbf{P}_\infty$ the sensor set with the lowest entry.
3. Combine those selected sensor sets to obtain a larger initial sensor set to be reduced in the subsequent sequential greedy selection phase.

This approach is motivated by two reasons.

1. While working with sensor sets adds complexity compared to working with individual sensors, sensor sets of minimum size (smaller than the final size of the optimized sensor set) are still manageable. They allow for the fastest evaluation of $\mathbf{P}_\infty$ and limit the number of potential sensor sets to explore, which grows with the factorial of the size of the sensor sets. Still, exhaustive exploration is not possible, but random sampling gives reasonable results thanks to the size reduction.
2. Using this random sampling, finding a sensor set which simultaneously provides acceptable performance for all quantities to estimate is computationally challenging. However, separately finding sensor sets with acceptable performance for each quantity to estimate is manageable. These sensor sets can then be combined to obtain an initial sensor set that performs well for all quantities to estimate, thanks to property (6) where inequality $\mathbf{A} < \mathbf{B}$ is in the strict sense $\lambda_{\mathbf{A},i} < \lambda_{\mathbf{B},i} \ \ \forall i = 1, ..., n$.

$$\begin{aligned} \mathbf{P}_\infty(\mathbf{S}_a \cup \mathbf{S}_b) &< \mathbf{P}_\infty(\mathbf{S}_a) \\ &< \mathbf{P}_\infty(\mathbf{S}_b) \end{aligned} \tag{6}$$

The approach described above provides a sensor set of manageable size and with good $\mathbf{P}_\infty$ that is suited for the final sequential greedy reduction phase that follows.

3.3 Sequential Greedy reduction phase

In this final phase, sensors are sequentially removed from the large initial sensor set. Each iteration removes the sensor of which the removal reduces the performance the least, and this is repeated until either a performance threshold is reached or a cost objective is met.

To measure and compare performance, multiple functions Ψ have been used to summarize $\mathbf{P}_\infty$ into a single scalar quantifying the uncertainty ellipsoid around the estimated state [25]:

$$\Psi_A(\mathbf{P}_\infty) = \sqrt{\mathrm{trace}(\mathbf{P}_\infty)} \qquad \Psi_D(\mathbf{P}_\infty) = \ln(\det(\mathbf{P}_\infty)) \qquad \Psi_E(\mathbf{P}_\infty) = \lambda_{max}(\mathbf{P}_\infty))$$

Ψ_A is proportional to the mean squared length of the ellipsoid's axes, and is also related to the expected estimation Root Mean Square Error (RMSE), while Ψ_D represents the ellipsoid's volume, and Ψ_E the length of its largest axis. Because $\mathbf{P}_\infty$ is already a black-box function of the decision variables, the choice of Ψ is not driven by considerations of convexity or linearity. In this work, $\Psi_A(\mathbf{P}_\infty) = \sqrt{\mathrm{trace}(\mathbf{P}_\infty)}$ is chosen as the objective function to minimize.

The overall sensor selection flow is summarized in Figure 1.

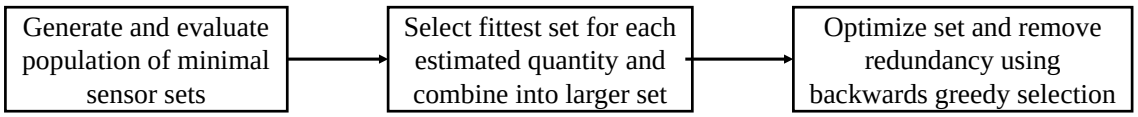

Figure 1: Sensor selection flow

4 Use-case model

This work applies the sensor selection approach presented above to the use-case of load estimation of a wind turbine pitch bearing. Before presenting the results, a short overview is given of the model underlying the virtual sensing work. An analytical model of the ball bearing itself is combined with a finite element (FE) model of the hub to obtain field variables (displacements, strains, accelerations, ...) on the hub as a response to the forces and torques exerted by the blade on the inner ring of the pitch bearing [27].

The ball bearing is modeled using an analytical bearing model based on Hertzian contact theory to describe the interactions between the rolling elements and the raceways. The bearing is a double-row, 4-points-of-contact deep groove ball bearing with $2.5\,\mathrm{m}$ pitch diameter. The analytical contact model allows to derive the forces distributed over the raceways of the outer ring corresponding to the bearing reaction forces which must balance the five components of the blade forces: three force components and two torque components (the bearing is considered to have no rolling resistance and the torque about the bearing axis is thus considered zero).

The hub is modeled using a reduced-order model based on FE Analysis, which uses those raceway forces as input. The dimensionality reduction is useful for virtual sensing because it makes the size of the state to

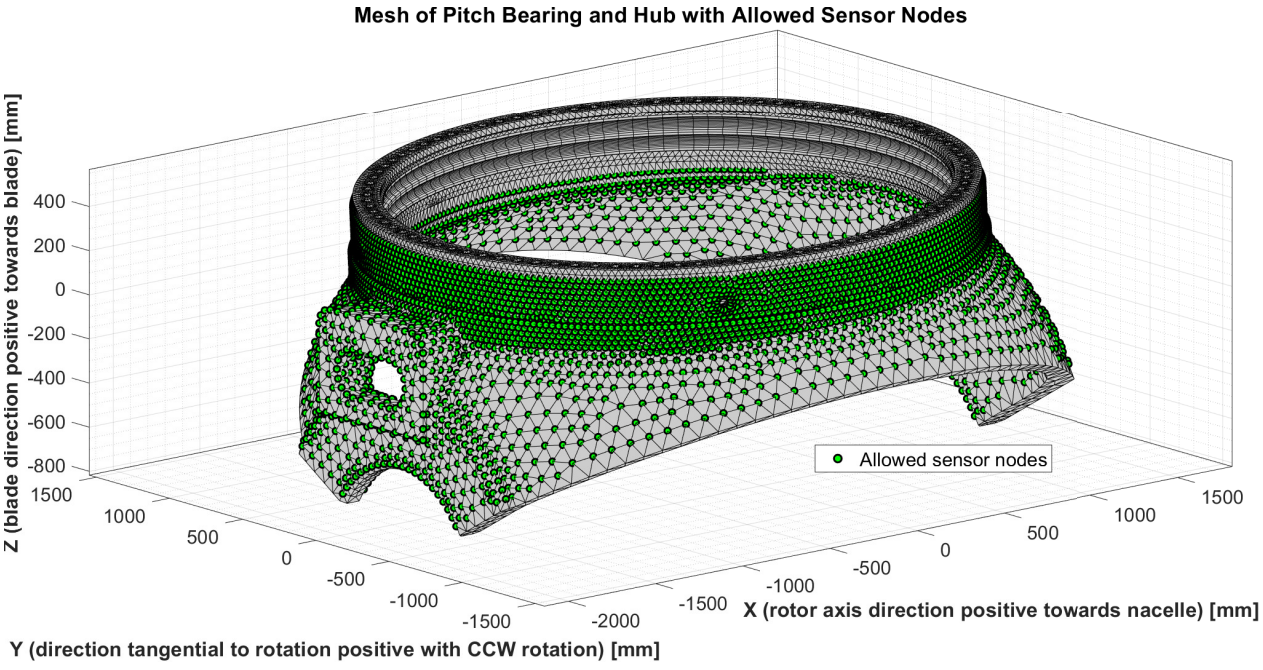

Figure 2: FE model of pitch bearing and hub, with allowed sensor positions

estimate manageable, and because it makes the bearing observable for a feasible number of sensors.

Figure 2 shows the general geometry of the hub and its FE mesh, along with the allowed sensor positions. Sensors can be placed at any nodes on the outer shell of the hub, but cannot be placed inside the bearings or on the face to which the blade is bolted for practical reasons. Sensors can be accelerometers or strain gauges. Each accelerometer measures three accelerations in the three axial directions, while each strain gauge measures two in-plane strains, in the hoop direction and in the axial direction. Table 1 summarizes the scale of the resulting sensor selection problem through some key parameters. Table 2 provides some characteristic dimensions of the considered use-case.

Table 1: Scale of the sensor selection problem

	Number of
Elements	128942
Modes	10
Nodes	42994
Shell Nodes	31513
Allowed sensor nodes	8475

Table 2: General scale of the pitch bearing use-case

Nameplate capacity	$3.4\,\mathrm{MW}$
Pitch diameter	$2.5\,\mathrm{m}$
Blade length	$50\,\mathrm{m}$
Blade weight	$15\,\mathrm{t}$

5 Results

Figure 3 presents the results of a sensor selection run, with the selection parameters listed in table 3.

Table 3: Sensor selection parameters

Population	10^5 sensor sets
# strain gauges per population set	5
# accelerometers per population set	5
Strain gauge noise std	10^{-7} mm def./mm mat.
Accelerometer noise std	$1\,\mathrm{mm\,s^{-2}}$
Final # strain gauges	10
Final # accelerometers	10

The number of strain gauges and accelerometers in the final set is chosen based on Figure 4 which shows how the estimation performance evolves as a function of the number of strain gauges and accelerometers. As expected, Figure 4 shows that performance always decreases (*i.e.* Ψ_A increases) with the removal of sensors. This loss of performance is not linear with the number of sensors and both an inflection point as well a ceiling on estimation performance can be seen.

The sensor sets resulting from the proposed sensor selection approach can be intuitively understood given that the hub is close to axisymmetrical. The sensors are placed close to the bearing raceways where the contact forces are transfer the blade forces, and they are distributed along the hub circumference. Moreover, the sensor positions are also consistent with regions of high deformation of the modeshapes selected in the model order reduction.

Table 4 summarizes the performance of the proposed sensor set and compares it to the performance of a sensor set based on simple geometrical heuristics as depicted in Figure 5. Table 4 shows that the optimized

Table 4: Estimation performance of the final set

	Uncertainty std [kN]	
Estimated quantity	Proposed	Heuristics-based
f_x	0.43	0.33
f_y	0.77	2.88
f_z	1.24	2.15
$\Psi_A \sim$ overall RMSE	1.52	3.61

sensor set indeed outperforms the hand-picked sensor set. The predicted uncertainties are consistent with error metrics obtained when actually running an estimator on the presented use-case.

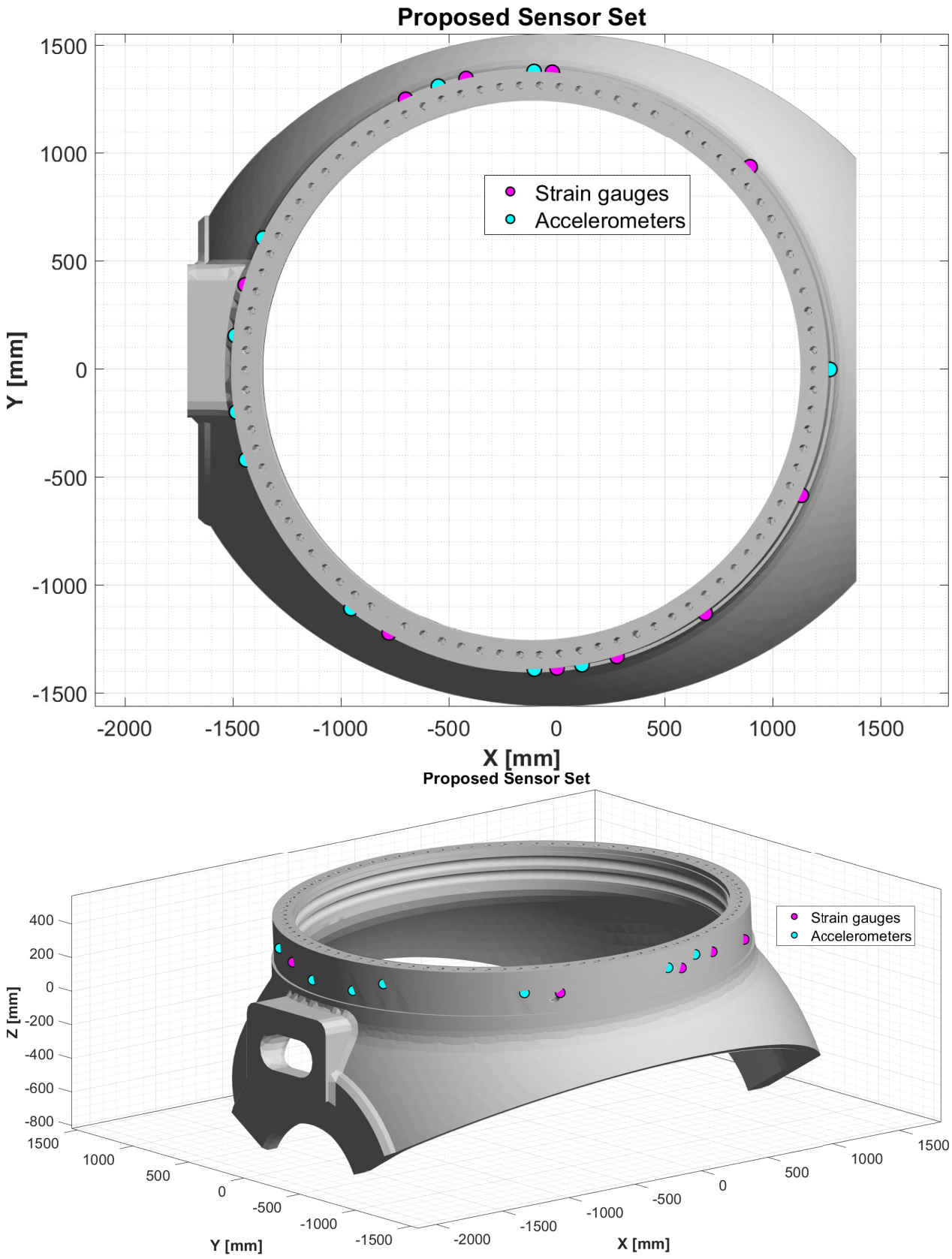

Figure 3: Proposed sensor set: top and side view

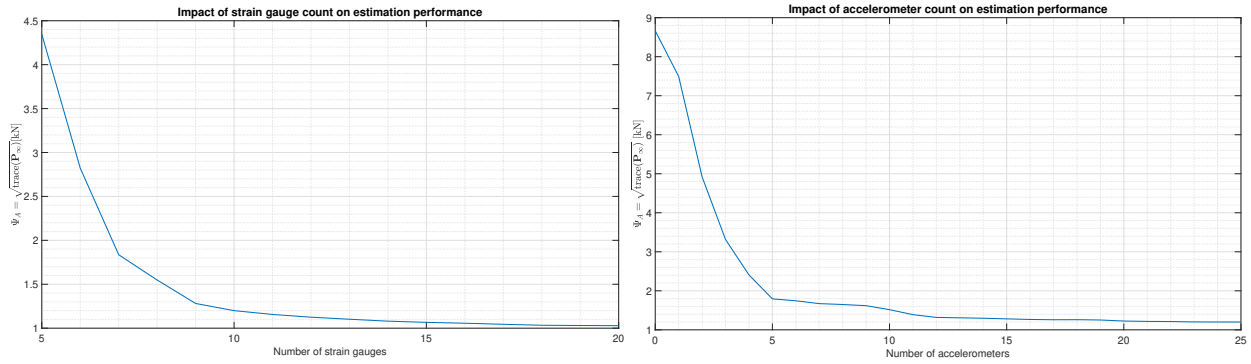

Figure 4: Estimation performance in function of number of sensors

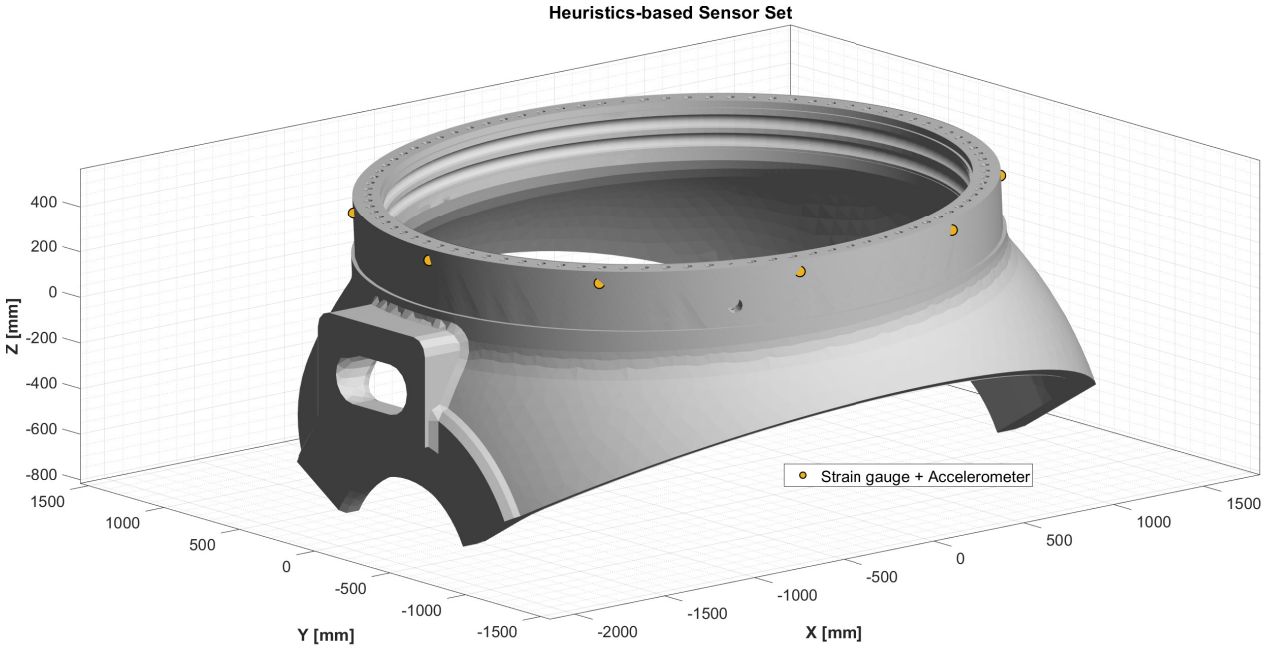

Figure 5: Heuristics-based sensor positions for comparison

6 Conclusions

In this article, a sensor selection method is proposed and applied to the use-case of load estimation of a wind turbine pitch bearing. This method allows to generate performant sensor sets without requiring the help domain-specific constraints and heuristics. Still, the selected positions remain consistent with the highly-excited regions of the hub and with common sensor selection intuitions. This also underlines the importance of the modelling steps that precede the sensor selection step. In particular, model order reduction is crucial for virtual sensing using FE-based models and the importance of the choice of reduction basis is clear.

The obtained sensor sets outperform hand-picked sensor sets that are often used in practice. Comparison to recently proposed sensor selection approaches [14] on standard test-cases has not been done, as this work focuses the wind turbine pitch bearing use-case. Standardized benchmarks on a library of estimation problems with available models and data would be valuable to the research community.

The proposed approach relies on the AKF framework to derive $\mathbf{P}_\infty$, the covariance matrix of the asymptotic uncertainty on the estimation, which is used as performance metric for a given sensor set. This article has presented the advantages of such an approach, but this approach also comes with the limitation that only sensor sets can be evaluated, and not individual sensors. To accommodate this, the defining aspect of the work presented here is the choice to always consider the performance of a given sensor set, or the contribution of an individual sensor to the performance of a given sensor set, but never the performance of an individual sensor in a vacuum, for which a rigorous metric is not available. The sensor selection procedure adopted in this work reflects this choice and relies on quasi Monte Carlo methods to handle the scale and complexity of the resulting sensor selection problem.

Still, this article has demonstrated how powerful a tool $\mathbf{P}_\infty$ is. It allows to quickly derive a metric for the performance of a given sensor set, based only on the model of the bearing and hub and on the positions and noise levels of the individual sensors. The metric is valid in all operating conditions where the model remains accurate, and does not require simulation results from one or more representative scenarios. This article has shown how this metric can also be used to choose the number of sensors and evaluate the evolution of the estimation performance in function of this number, which can be used for cost-benefit analyses.

Two further improvements are considered in the next steps. First, strain gauge orientation could be added as a decision variable to the sensor selection problem. Optimizing the orientation along with the position of the strain gauges is a natural extension of this work, but further increases the dimensionality of the optimization problem. Separation of the larger resulting sensor selection problem into smaller decoupled problems could be investigated to tackle this increased complexity.

Second, the presented approach could be extended to also take into account quality of the model at the sensor positions into the sensor selection. In this work, the $\mathbf{R}$ matrix is not a function of the sensor positions and only depends on the sensor noises. To account for areas of varying model accuracy or affected by non-linearities, this matrix could be made position-dependent in order to weigh each position according to the trustworthiness of the model predictions at that position.

Future work should also investigate how more refined optimization algorithms could be leveraged to accelerate or improve the sensor selection procedure. Topology optimization problems have a structure similar to the sensor selection problem considered here, and they could provide inspiration for methods to approximate $\mathbf{P}_\infty$ as a function of continuous variables instead of binary selection variables.This would allow to apply gradient-descent methods which have interesting optimality and convergence properties.

On the other side of the spectrum of optimization methods, genetic algorithms (GA) should also be considered to solve the sensor selection problem. The approach presented in this article already shares some aspects with GAs, and this is no surprise as a GA problem can be almost directly formulated from the sensor selection problem, with binary selection variables as genes and a fitness metric based on $\mathbf{P}_\infty$. Crossovers and mutations also make intuitive sense in the context of sensor selection. However, the scale of the problem might be a challenge requiring further research to make it amenable to this interesting class of evolutionary algorithms.

Acknowledgements

The European Commission is gratefully acknowledged for their support of the INNTERESTING research project (GA 851245) along with Internal Funds KU Leuven for their backing.

References

[1] P. Veers, K. Dykes, E. Lantz, S. Barth, C. L. Bottasso, O. Carlson, A. Clifton, J. Green, P. Green, H. Holttinen, D. Laird, V. Lehtomäki, J. K. Lundquist, J. Manwell, M. Marquis, C. Meneveau, P. Moriarty, X. Munduate, M. Muskulus, J. Naughton, L. Pao, J. Paquette, J. Peinke, A. Robertson, J. Sanz Rodrigo, A. M. Sempreviva, J. C. Smith, A. Tuohy, and R. Wiser, "Grand challenges in the science of wind energy," *Science*, vol. 366, no. 6464, p. eaau2027, Oct. 2019. [Online]. Available: https://doi.org/10.1126/science.aau2027

[2] M. I. Blanco, "The economics of wind energy," *Renewable and Sustainable Energy Reviews*, vol. 13, no. 6, pp. 1372–1382, Aug. 2009. [Online]. Available: https://doi.org/10.1016/j.rser.2008.09.004

[3] M. Shafiee and J. D. Sørensen, "Maintenance optimization and inspection planning of wind energy assets: Models, methods and strategies," *Reliability Engineering & System Safety*, vol. 192, p. 105993, Dec. 2019. [Online]. Available: https://doi.org/10.1016/j.ress.2017.10.025

[4] W. Zhou, T. G. Habetler, and R. G. Harley, "Bearing Condition Monitoring Methods for Electric Machines: A General Review," in *2007 IEEE International Symposium on Diagnostics for Electric Machines, Power Electronics and Drives*, Sep. 2007, pp. 3–6. [Online]. Available: https://doi.org/10.1109/DEMPED.2007.4393062

[5] C. Malla and I. Panigrahi, "Review of Condition Monitoring of Rolling Element Bearing Using Vibration Analysis and Other Techniques," *Journal of Vibration Engineering & Technologies*, vol. 7, no. 4, pp. 407–414, Aug. 2019. [Online]. Available: https://doi.org/10.1007/s42417-019-00119-y

[6] H. D. M. de Azevedo, A. M. Araújo, and N. Bouchonneau, "A review of wind turbine bearing condition monitoring: State of the art and challenges," *Renewable and Sustainable Energy Reviews*, vol. 56, pp. 368–379, Apr. 2016. [Online]. Available: https://doi.org/10.1016/j.rser.2015.11.032

[7] A. Reedman, "Bearing monitoring using a fiber Bragg grating," U.S. Patent US9 014 518B2, Apr., 2015.

[8] L. Hoffmann, M. S. Mueller, and A. W. Koch, "Fiber optic strain measurement for machine monitoring," in *Optical Measurement Systems for Industrial Inspection V*, vol. 6616. SPIE, Jun. 2007, pp. 953–961. [Online]. Available: https://doi.org/10.1117/12.726026

[9] B. J. Dobson and E. Rider, "A review of the indirect calculation of excitation forces from measured structural response data," *Proceedings of the Institution of Mechanical Engineers, Part C: Mechanical Engineering Science*, vol. 204, no. 2, pp. 69–75, 1990. [Online]. Available: https://doi.org/10.1243/PIME_PROC_1990_204_080_02

[10] R. Adams and J. F. Doyle, "Multiple force identification for complex structures," *Experimental Mechanics*, vol. 42, no. 1, pp. 25–36, Mar. 2002. [Online]. Available: https://doi.org/10.1007/BF02411048

[11] M. V. van der Seijs, D. de Klerk, and D. J. Rixen, "General framework for transfer path analysis: History, theory and classification of techniques," *Mechanical Systems and Signal Processing*, vol. 68-69, pp. 217–244, Feb. 2016. [Online]. Available: https://doi.org/10.1016/j.ymssp.2015.08.004

[12] R. E. Kalman, "A new approach to linear filtering and prediction problems," *Transactions of the ASME–Journal of Basic Engineering*, vol. 82, no. Series D, pp. 35–45, 1960.

[13] E. Lourens, E. Reynders, G. De Roeck, G. Degrande, and G. Lombaert, "An augmented Kalman filter for force identification in structural dynamics," *Mechanical Systems and Signal Processing*, vol. 27, pp. 446–460, Feb. 2012. [Online]. Available: https://doi.org/10.1016/j.ymssp.2011.09.025

[14] R. Cumbo, L. Mazzanti, T. Tamarozzi, P. Jiranek, W. Desmet, and F. Naets, "Advanced optimal sensor placement for Kalman-based multiple-input estimation," *Mechanical Systems and Signal Processing*, vol. 160, p. 107830, Nov. 2021. [Online]. Available: https://www.sciencedirect.com/science/article/pii/S0888327021002259

[15] T. Tamarozzi, E. Risaliti, W. Rottiers, K. Janssens, and W. Desmet, "Noise, ill-conditioning and sensor placement analysis for force estimation through virtual sensing," p. 15.

[16] T. Devos, M. Kirchner, J. Croes, W. Desmet, and F. Naets, "Sensor Selection and State Estimation for Unobservable and Non-Linear System Models," *Sensors*, vol. 21, no. 22, p. 7492, Jan. 2021, number: 22 Publisher: Multidisciplinary Digital Publishing Institute. [Online]. Available: https://www.mdpi.com/1424-8220/21/22/7492

[17] C. Cappelle, M. Cattebeke, J. Bosmans, M. Kirchner, J. Croes, and W. Desmet, "Sensor selection for cost-effective virtual torque measurements on a wind turbine gearbox," *Forschung im Ingenieurwesen*, vol. 85, no. 2, pp. 325–334, Jun. 2021. [Online]. Available: https://doi.org/10.1007/s10010-021-00464-z

[18] X. Iriarte, J. Aginaga, F. Lerga, G. Gainza, J. Ros, and J. Bacaicoa, "Optimal strain gauge configurations for the estimation of mechanical loads in the main shaft of HAWT," *Journal of Physics: Conference Series*, vol. 1618, no. 2, p. 022034, Sep. 2020. [Online]. Available: https://iopscience.iop.org/article/10.1088/1742-6596/1618/2/022034

[19] M. Khalil, I. Kouroudis, R. Wüchner, and K.-U. Bletzinger, "Optimal Sensor Configuration for Fatigue Life Prediction in Structural Applications." American Society of Mechanical Engineers Digital Collection, Nov. 2019. [Online]. Available: https://asmedigitalcollection.asme.org/DSCC/proceedings/DSCC2019/59148/V001T06A001/1070456

[20] L. Mazzanti, R. Cumbo, W. Desmet, F. Naets, and T. Tamarozzi, "An Improved Optimal Sensor Placement Strategy for Kalman-Based Multiple-Input Estimation," in *Model Validation and Uncertainty Quantification, Volume 3*, ser. Conference Proceedings of the Society for Experimental Mechanics Series, Z. Mao, Ed. Cham: Springer International Publishing, 2020, pp. 181–185.

[21] R. G. Brown and P. Y. C. Hwang, *Introduction to random signals and applied Kalman filtering: with MATLAB exercises and solutions*, 3rd ed. New York: Wiley, 1997.

[22] S. J. Julier and J. K. Uhlmann, "New extension of the Kalman filter to nonlinear systems," I. Kadar, Ed., Orlando, FL, USA, Jul. 1997, p. 182. [Online]. Available: http://proceedings.spiedigitallibrary.org/proceeding.aspx?doi=10.1117/12.280797

[23] S. Eftekhar Azam, E. Chatzi, and C. Papadimitriou, "A dual Kalman filter approach for state estimation via output-only acceleration measurements," *Mechanical Systems and Signal Processing*, vol. 60-61, pp. 866–886, Aug. 2015. [Online]. Available: https://www.sciencedirect.com/science/article/pii/S0888327015000746

[24] D. Simon, *Optimal state estimation: Kalman, H [infinity] and nonlinear approaches*. Hoboken, N.J: Wiley-Interscience, 2006, oCLC: ocm64084871.

[25] P. Benner, R. Herzog, N. Lang, I. Riedel, and J. Saak, "Comparison of model order reduction methods for optimal sensor placement for thermo-elastic models," *Engineering Optimization*, vol. 51, no. 3, pp. 465–483, Mar. 2019, publisher: Taylor & Francis _eprint: https://doi.org/10.1080/0305215X.2018.1469133. [Online]. Available: https://doi.org/10.1080/0305215X.2018.1469133

[26] S. Kucherenko, "Application of Quasi Monte Carlo Methods in Global Optimization," in *Global Optimization: From Theory to Implementation*, ser. Nonconvex Optimization and Its Applications, L. Liberti and N. Maculan, Eds. Boston, MA: Springer US, 2006, pp. 111–133. [Online]. Available: https://doi.org/10.1007/0-387-30528-9_5

[27] N. Cappellini, T. Tamarozzi, B. Blockmans, J. Fiszer, F. Cosco, and W. Desmet, "Semi-analytic contact technique in a non-linear parametric model order reduction method for gear simulations," *Meccanica*, vol. 53, no. 1-2, pp. 49–75, Jan. 2018. [Online]. Available: https://doi.org/10.1007/s11012-017-0710-5